

# Nanoparticles Modified With Tumor-targeting scFv Deliver siRNA and miRNA for Cancer Therapy

Yunching Chen<sup>1</sup>, Xiaodong Zhu<sup>2</sup>, Xiaoju Zhang<sup>2</sup>, Bin Liu<sup>2</sup> and Leaf Huang<sup>1</sup>

<sup>1</sup>Division of Molecular Pharmaceutics, Eshelman School of Pharmacy, University of North Carolina at Chapel Hill, Chapel Hill, North Carolina, USA;

<sup>2</sup>Helen Diller Family Comprehensive Cancer Center, University of California at San Francisco, San Francisco, California, USA

Targeted delivery of RNA-based therapeutics for cancer therapy remains a challenge. We have developed a LPH (liposome-polycation-hyaluronic acid) nanoparticle formulation modified with tumor-targeting single-chain antibody fragment (scFv) for systemic delivery of small interfering RNA (siRNA) and microRNA (miRNA) into experimental lung metastasis of murine B16F10 melanoma. The siRNAs delivered by the scFv targeted nanoparticles efficiently downregulated the target genes (c-Myc/MDM2/VEGF) in the lung metastasis. Two daily intravenous injections of the combined siRNAs in the GC4-targeted nanoparticles significantly reduced the tumor load in the lung. miRNA-34a (miR-34a) induced apoptosis, inhibited survivin expression, and downregulated MAPK pathway in B16F10 cells. miR-34a delivered by the GC4-targeted nanoparticles significantly downregulated the survivin expression in the metastatic tumor and reduced tumor load in the lung. When miR-34a and siRNAs were co-formulated in GC4-targeted nanoparticles, an enhanced anticancer effect was observed.

Received 10 February 2010; accepted 5 June 2010; published online 6 July 2010. doi:10.1038/mt.2010.136

## INTRODUCTION

RNA-based therapeutics such as small interfering RNA (siRNA) and microRNA (miRNA) provide a promising strategy to treat cancer by targeting the specific proteins involved in the mechanism of proliferation, invasion, antiapoptosis, drug resistance, and metastasis.<sup>1–3</sup> Our previous study demonstrated that a combination of siRNAs against c-Myc, MDM2, and vascular endothelial growth factor (VEGF) co-formulated in the targeted nanoparticles significantly reduced the lung metastasis and increased the survival time of the tumor-bearing animals.<sup>4</sup> miR-34a, a potential tumor suppressor in many types of human cancers including melanoma, was selected as a therapeutic target in this study. miR-34a is commonly downregulated in many human cancers.<sup>5</sup> Multiple mechanisms are involved in the anticancer effect of miR-34a. For example, miR-34a inhibits the proliferation and migration and triggers apoptosis in some cancer cell lines via the activation of p53 and downregulation of c-Met.<sup>6,7</sup> It also directly targets the

mRNA encoding E2F3 and significantly suppresses the expression of E2F3 protein, a key regulator of cell cycle progression.<sup>8</sup> The activity of survivin promoter is decreased after the treatment of miR-34a.<sup>5</sup> Taken together, we hypothesize that miR-34a may serve as a suitable anticancer therapeutic agent.

The key to develop RNA-based therapeutics is to have effective strategies for the delivery of siRNA or miRNA *in vivo*.<sup>9</sup> For example, modification of antisense RNA with a cholesterol functionality results in enhanced stability in the serum, improved cellular uptake and inhibition of target mRNA.<sup>10</sup> Our strategy is to develop a nanoparticle formulation to deliver siRNA *in vivo*.<sup>4,11,12</sup> Recently, we further demonstrated liposome-polycation-hyaluronic acid (LPH) containing hyaluronic acid (HA), a US Food and Drug Administration-approved drug, could systemically deliver siRNA into the tumor with relatively low toxicity compared with the well-established LPD (liposome-polycation-DNA) formulation. However, the therapeutic effect of the LPH nanoparticles has not been tested.

In this study, we have modified LPH nanoparticles with GC4 single-chain variable fragment (scFv), a tumor-targeting human monoclonal antibody,<sup>13</sup> to effectively deliver siRNA and miRNA to B16F10 lung metastasis in a syngeneic murine model. As a targeting ligand, scFv shows high affinity and low antigenicity in previous studies.<sup>14,15</sup> We hypothesize that GC4 scFv will target the nanoparticles to tumor metastasis and deliver siRNA and miRNA intracellularly to metastatic tumor cells to inhibit their growth. The hypothesis was tested by using a combination of three different siRNAs and miR-34a.

## RESULTS

### Human scFv targeting B16F10 cells

To identify human scFvs that target B16F10 murine melanoma cells, we screened a panel of internalizing scFvs previously identified in our laboratory for binding to a panel of human tumor cells and cell lines. We found that the GC4 scFv, originally isolated for targeting human glioma tumor sphere cells,<sup>13</sup> binds to B16F10 cell lines (Figure 1a). The GC4 scFv thus recognizes an epitope conserved between mouse and human. Because of its well-characterized internalizing functions,<sup>13</sup> we have chosen this scFv to develop nanosized vehicles for systemic delivery of RNA therapeutics to B16F10 cells.

**Correspondence:** Bin Liu, Helen Diller Family Comprehensive Cancer Center, Box 1371, University of California at San Francisco, San Francisco, California 94143, USA. E-mail: liub@anesthesia.ucsf.edu or Leaf Huang, Division of Molecular Pharmaceutics, Eshelman School of Pharmacy, Campus Box 7571, Kerr Hall, University of North Carolina at Chapel Hill, Chapel Hill, North Carolina 27599, USA. E-mail: leafh@unc.edu

## Production and purification of GC4 scFv with a free C-terminal cysteine

The gene encoding the GC4 scFv was spliced into a bacteria expression vector to create an in-frame fusion with the amino acid cysteine and the hexahistidine tag. Antibody was purified from bacterial periplasmic space by IMAC and analyzed on SDS-PAGE under nonreducing and reducing conditions (Figure 1b). Approximately 50% of the total antibody fragments initially purified from bacteria periplasmic space were in dimeric form. After reduction, over 90% of antibody fragments were in monomeric form.

## Delivery of siRNA by using GC4 scFv modified nanoparticles

The LPH nanoparticles were self-assembled by charge-charge interaction. A slight excess amount of HA and siRNA or miRNA was first complexed with protamine such that the condensed cores were negatively charged. The complex was then encapsulated by cationic liposomes composed of DOTAP/cholesterol (1:1 mol/mol) via charge interaction. The nanoparticles were further PEGylated and modified with the tumor-targeting GC4 scFv to increase the stability of the formulation in the blood circulation and selectively deliver the cargo into the tumor cells, respectively. The average size of the nanoparticles modified with GC4 scFv was about 170 nm and the zeta potential was  $10.9 \pm 4.8$  mV. As shown in Figure 2a, the uptake of fluorescein isothiocyanate (FITC)-labeled siRNA was greater in B16F10 cells treated with GC4-targeted nanoparticles than cells treated with control-targeted nanoparticles. As shown in Supplementary Figure S1,

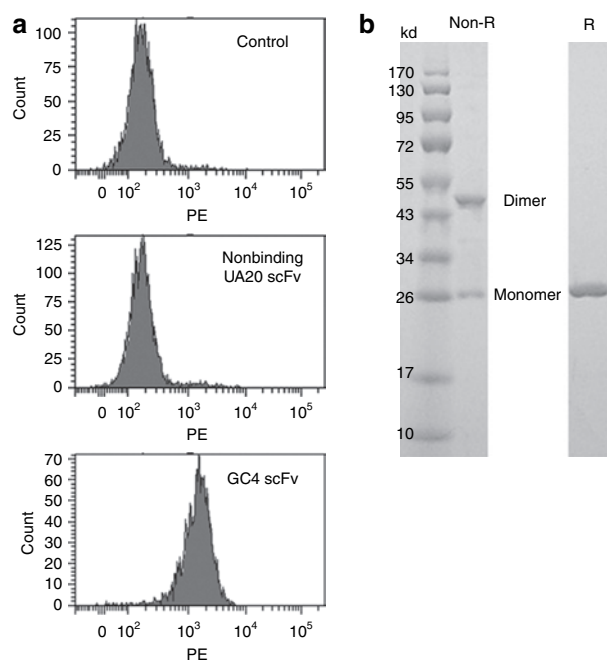


**Figure 1** Binding of recombinant GC4 scFv to B16F10 cells. **(a)** FACS screening of scFvs binding to B16F10 cells. The GC4 scFv binds but not other scFvs studied (e.g., UA20). Control: B16F10 cells incubated with secondary detection reagents only. **(b)** Analysis of recombinant GC4 scFv by gel electrophoresis under nonreducing (non-R) and reducing (R) conditions. Dimer and monomer (reduced scFv) are indicated. PE, phycoerythrin.

the cy3-labeled siRNA appeared in both the surface and the cytoplasm of the cells (Supplementary Materials and Methods). The result indicates that GC4 scFv enhanced intracellular uptake of the nanoparticles for B16F10 cells.

We further studied the FITC-labeled siRNA uptake in the B16F10 lung metastasis in the tumor-bearing mice 4 hours after i.v. injection using confocal microscopy. As shown in Figure 2b, the intracellular fluorescence signals were hardly detected in the tumor tissues collected from the mice treated with free siRNA. The GC4-targeted nanoparticles showed strong cytosolic delivery of FITC-siRNA in the tumor tissue. In other organs (Figure 2c), the liver and the kidney showed higher uptake of free siRNA than siRNA formulated in the GC4-targeted nanoparticles, whereas the GC4-targeted nanoparticles showed stronger siRNA uptake in the tumor nodules in the lung than free siRNA. The results demonstrate that GC4-targeted nanoparticles enhanced uptake of siRNA in B16F10 lung metastasis.

## In vivo gene silencing study

To further investigate the biological activity of the nanoparticles *in vivo*, combined siRNAs against c-Myc, MDM2, and VEGF

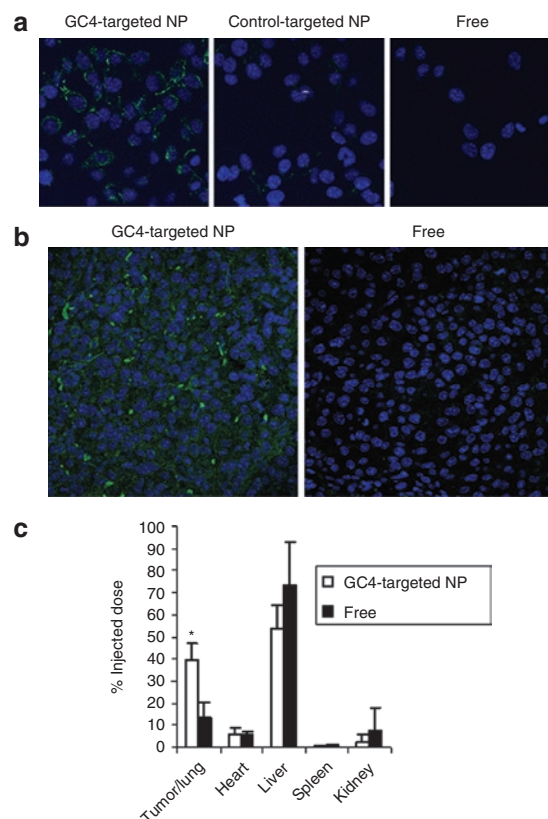


**Figure 2** Uptake of siRNA *in vitro* and *in vivo*. **(a)** Fluorescence photographs of B16F10 cells after treatment with free siRNA or siRNA formulated in the GC4-targeted or control-targeted nanoparticles (NPs) for 1 hour. Fluorescence signal of FITC-labeled siRNA in B16F10 cells was observed by the confocal microscopy. **(b)** Fluorescence signal of FITC-labeled siRNA in B16F10 metastasis nodules observed by confocal microscopy. **(c)** Comparative tissue distribution of FITC-labeled siRNA in tumor-bearing mice 4 hours after injection of either free siRNA or siRNA formulated in the GC4-targeted NPs, expressed as percent of the injected siRNA in the whole organ. Data = mean  $\pm$  SD,  $n = 3$ . \* $P < 0.05$  compared with free siRNA.

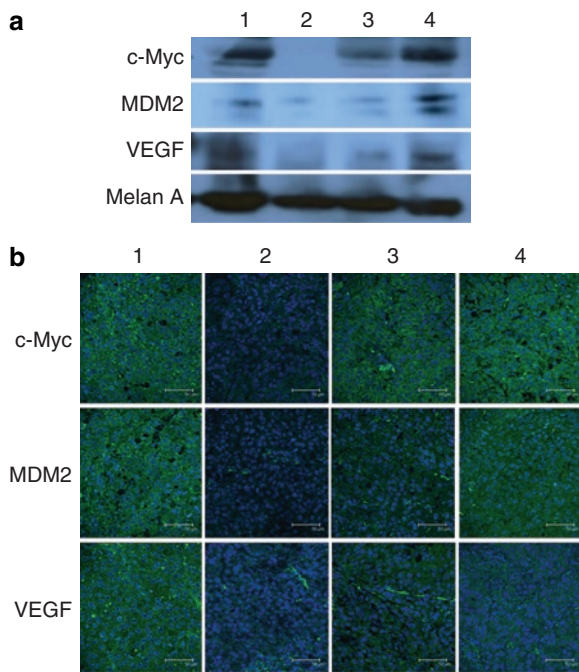


**Figure 3** Protein expression in B16F10 tumor-bearing lung. **(a)** Western blot analysis and **(b)** immunostaining of c-Myc, VEGF, and MDM2 in the lungs containing B16F10 metastasis nodules after i.v. injections of combined siRNAs in different formulations. Bar = 50  $\mu$ m. Formulations: untreated control (1), combined siRNAs in the GC4-targeted nanoparticles (2), combined siRNAs in the control-targeted nanoparticles (3), and control siRNA in the GC4-targeted nanoparticles (4).

(1:1:1 weight ratio) were delivered by either GC4-targeted or control-targeted nanoparticles. The B16F10 lung metastasis-bearing mice were treated with different formulations on days 10 and 11 with two consecutive i.v. administrations (dose = 0.45 mg total siRNA/kg). The gene silencing activity was determined by western blot analysis and immunostaining (Figure 3). As shown in the figures, the protein expression of c-Myc, MDM2, and VEGF in the B16F10 lung metastasis was suppressed by the combined siRNAs delivered with GC4-targeted nanoparticles. The control-targeted nanoparticles showed a partial gene silencing effect, whereas the control siRNA delivered by GC4-targeted nanoparticles had no effect. The results indicate that the combined siRNAs formulated in the targeted nanoparticles modified with GC4 scFv were able to simultaneously silence the expressions of the target oncogenes in the lung metastases.

### Tumor growth/metastasis inhibition by siRNA nanoparticles

To elucidate the therapeutic outcomes, the lung metastasis-bearing mice were treated with different formulations on days 8 and 9 with two consecutive i.v. administrations (dose = 0.45 mg total siRNA/kg). As shown in Figure 4a, the growth of the metastasis nodules in the lung was significantly inhibited when treated with the combined siRNAs formulated in the targeted nanoparticles modified with GC4 scFv. Other control groups treated with the combined siRNAs formulated in the control-targeted nanoparticles and the control siRNA formulated in GC4-targeted nanoparticles had no therapeutic effect. Furthermore, because

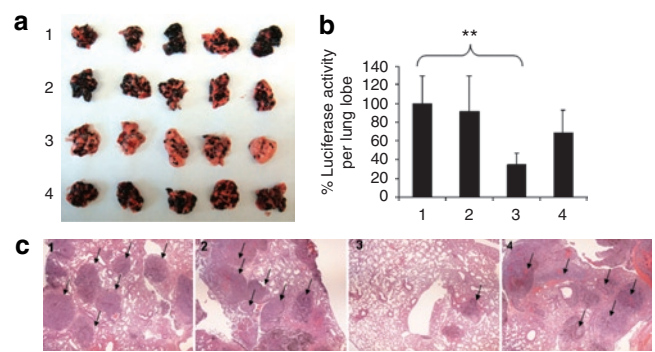


**Figure 4** Tumor growth/metastasis inhibition by nanoparticles containing siRNA. **(a)** Images of the B16F10 tumor-bearing lung on day 19 after two consecutive i.v. injections of siRNAs in different formulations. **(b)** Luciferase activity in the tumor-bearing lung on day 19 after two consecutive i.v. injections on days 8 and 9 of siRNA in different formulations.  $n = 5$ .  $**P < 0.01$  as compared to the untreated group. **(c)** Photographs of the hematoxylin and eosin-stained tissue sections of B16F10 tumor-bearing lung on day 19 after two consecutive i.v. injections of siRNAs in different formulations. Solid arrows indicate the tumor nodules in the lungs. NPs, nanoparticles. Formulations: untreated control (1), combined siRNAs in the control-targeted nanoparticles (2), combined siRNAs in the GC4-targeted nanoparticles (3), and control siRNA in the GC4-targeted nanoparticles (4).

B16F10 cells were stably transfected with firefly luciferase gene, the B16F10 lung metastases were further quantified by measuring the luciferase activity in the lung. As shown in Figure 4b, the combined siRNAs delivered by the GC4-targeted nanoparticles suppressed the growth of the metastasis nodules; the tumor load decreased to about 30% of the untreated control ( $P < 0.01$ ). Other control treatments showed no obvious therapeutic effect. The hematoxylin and eosin-stained tissue sections (Figure 4c) also showed a reduction in size and number of the metastasis nodules in the lung after treatment with the combined siRNAs formulated in the GC4-targeted nanoparticles, whereas other control groups showed no significant therapeutic effect. The results indicate that the combined siRNAs delivered by GC4-targeted nanoparticles could inhibit the growth of B16F10 lung metastasis.

### Downregulation of survivin expression and MAPK signaling by miR-34a

Both survivin and MAPK signaling play important roles in melanoma development and progression and are regulated by miR-34a in some cancer cells.<sup>5,16-19</sup> To test the specific regulation of survivin and MAPK signaling, B16F10 cells were transfected with miR-34a or a control miRNA. As shown in Figure 5a, western blot analysis showed that both survivin and pERK expressions were significantly downregulated when B16F10 cells were treated with miR-34a, whereas the control miRNA had no effect. To further investigate the biological activity of miR-34a *in vivo*, miR-34a was delivered by either GC4-targeted or control-targeted nanoparticles. The lung metastases-bearing mice were treated with different formulations on days 10 and 11 with two consecutive i.v. administrations (dose = 0.3 mg RNA/kg). The gene silencing activity was determined by western blot analysis. As shown in Figure 5b, the protein expression of survivin in the B16F10 lung metastasis was suppressed by miR-34a delivered with the



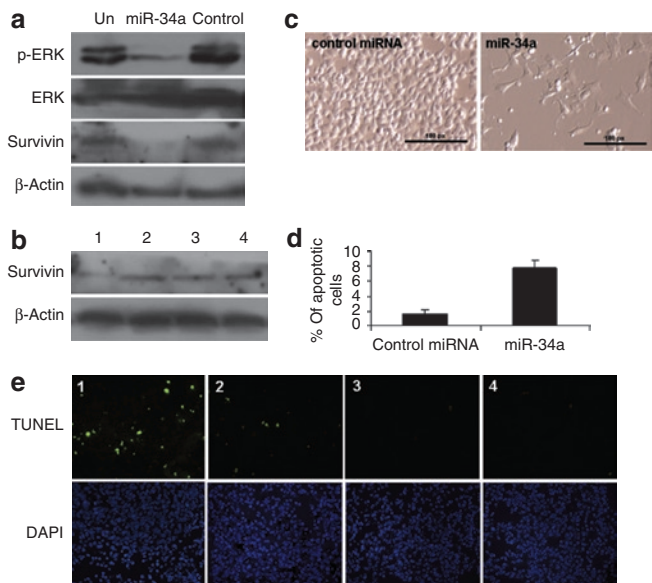


**Figure 5** Apoptosis induction and target gene downregulation by miR-34a. **(a)** Survivin and pERK expression in B16F10 cells 72 hours after transfection with miR-34a or a control miRNA. **(b)** Western blot analysis of survivin expression in lungs containing B16F10 metastatic nodules after i.v. injections of the miRNAs in different formulations. **(c)** Cell morphology 3 days after transfection with miR-34a or the control miRNA. **(d)** B16F10 cells transfected with miR-34a or a control miRNA for 72 hours and analyzed for annexin V staining by flow cytometry. **(e)** TUNEL staining of B16F10 lung metastases on day 12 after two consecutive i.v. injections on days 10 and 11 of miRNAs in different formulations. Bar = 100  $\mu$ m. Formulations: miR-34a in the GC4-targeted nanoparticles (1), miR-34a in the control-targeted nanoparticles (2), control miRNA in the GC4-targeted nanoparticles (3), and untreated control (4).

GC4-targeted nanoparticles. Neither the control-targeted nanoparticles containing miR-34a nor the control miRNA delivered by GC4-targeted nanoparticles showed any silencing effect. These results indicate that delivery of miR-34a inhibited the survivin expression and inactivated MAPK pathway, thus inducing apoptosis in the B16F10 melanoma.

### Apoptosis induction by miR-34a

We further determined the biological function of miR-34a on cell survival on highly metastatic B16F10 cells. Annexin V staining was carried out to detect apoptosis 72 hours after transfection. miR-34a triggered cell death, as observed by cell morphology (Figure 5c). As shown in Figure 5d, apoptosis was induced after the treatment with miR-34a compared with the control miRNA. To further evaluate apoptosis induction by miR-34a in the B16F10 lung metastasis tumor, we examined cellular apoptosis by using the TdT dUTP nick end-labeling (TUNEL) staining (Figure 5e). As shown in the figure, the number of TUNEL-positive cells increased after intravenous injections of miR-34a formulated in the GC4-targeted nanoparticles. Intravenous injections of miR-34a in the control-targeted nanoparticles showed a slight increase in TUNEL-positive cells. No significant apoptosis induction was observed in other treatment groups. These results suggested that miR-34a triggered cell death and might play a critical role in regulating the survival of B16F10 melanoma cells *in vitro* and *in vivo*.

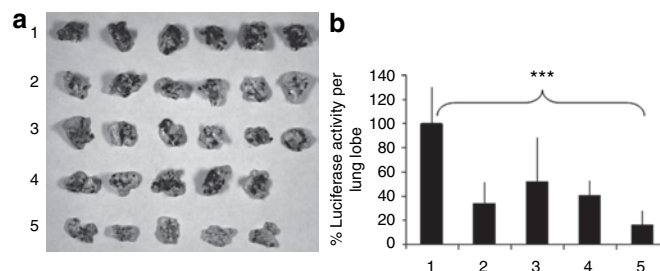


**Figure 6** Tumor growth/metastasis inhibition by nanoparticles containing siRNA and miRNA. **(a)** Images of the B16F10 tumor-bearing lungs on day 19 after two consecutive i.v. injections of siRNAs or miRNA in different formulations. **(b)** Luciferase activity in the tumor-bearing lungs on day 19 after two consecutive i.v. injections on days 8 and 9 of siRNAs and miRNA in different formulations.  $n = 5-6$ . \*\*\* $P < 0.001$ . Formulations: untreated control (1), combined siRNAs and control miRNA in the GC4-targeted nanoparticles (2), control siRNA and miR-34a in the GC4-targeted nanoparticles (3), combined siRNAs and miR-34a in the control-targeted nanoparticles (4), and combined siRNAs and miR-34a in the GC4-targeted nanoparticles (5). Dose = 0.6 mg total RNA/kg. Combined siRNAs = c-Myc:MDM2:VEGF (1:1:1), siRNA:miRNA = 1:1, weight ratios.

### Tumor growth/metastasis inhibition by nanoparticles containing siRNA and miRNA

To elucidate the therapeutic effect of the combination of siRNAs and miRNA, the lung metastasis-bearing mice were treated with different formulations on days 8 and 9 with two consecutive i.v. administrations (dose = 0.6 mg/kg, c-Myc:MDM2:VEGF:miR-34a = 1:1:1:3, weight ratio). As shown in Figure 6a, i.v. injections of siRNAs or miR-34a alone in the GC4-targeted nanoparticles showed a partial inhibition of the tumor load in the lung. The presence of the metastasis nodules was more significantly inhibited when treated with siRNAs and miR-34a co-formulated in the GC4-targeted nanoparticles. siRNAs and miR-34a co-delivered by the control-targeted nanoparticles had a partial therapeutic effect. B16F10 lung metastasis was further quantified by measuring luciferase activity in the lung. As shown in Figure 6b, siRNAs and miRNA-34a co-delivered by the GC4-targeted nanoparticles additively suppressed the growth of the metastasis tumor; the tumor load decreased to about 20% of the untreated control ( $P < 0.001$ ). It was reduced to about 30 and 50% when treated with siRNAs and miR-34a alone, respectively ( $P < 0.01$ ). The results indicated that the combination of siRNAs and miR-34a co-delivered by GC4-targeted nanoparticles could additively inhibit tumor growth and enhance the therapeutic effect in B16F10 lung metastasis model.

### Toxicity study

In addition to therapeutic effect, toxicity is a crucial parameter of a therapeutic agent for clinical use. The proinflammatory cytokines (IL-6, IL-12, and IFN- $\gamma$ ) and hepatotoxicity makers (aspartate aminotransferase and alanine aminotransferase) in the serum were examined in C57BL/6 mice for evaluation of toxicity induced by the nanoparticles (Table 1). miRNA and siRNA formulated in the GC4-targeted nanoparticles did not induce IL-6, IL-12, and IFN- $\gamma$  significantly. Aspartate aminotransferase and alanine aminotransferase levels also remained the same as the untreated animals. However, miRNA and siRNA formulated in the non-PEGylated nanoparticles induced a significant

**Table 1** Toxicity profile of nanoparticles

Cytokines or liver enzymes	No treatment (n = 5)	Treatment with non-PEGylated nanoparticles (n = 4)	Treatment with GC4-targeted nanoparticles (n = 4)
IL-6 (pg/ml)	310 ± 80	1,894 ± 239*	297 ± 81
IL-12 (pg/ml)	876 ± 112	1,785 ± 530*	1,063 ± 329
IFN- $\gamma$	ND	107 ± 35*	ND
AST (U/l)	24 ± 5	31 ± 5	28 ± 3
ALT (U/l)	57 ± 10	60 ± 10	59 ± 4

**Abbreviations:** ALT, alanine aminotransferase; AST, aspartate aminotransferase; IFN- $\gamma$ , interferon- $\gamma$ ; IL-6, interleukin-6; IL-12, interleukin-12; ND, not detectable. Sera of C57BL/6 mice were collected 4 hours after i.v. injections of combined siRNAs (0.3 mg/kg) and miR-34a (0.3 mg/kg) in the non-PEGylated nanoparticles or GC4-targeted nanoparticles for cytokine assays and 24 hours after treatments for evaluation of liver enzyme levels. Combined siRNAs = c-Myc:MDM2:VEGF (1:1:1). Data are shown as mean values  $\pm$  SD. \* $P < 0.01$ .

production of proinflammatory cytokine. The results indicate that the GC4-targeted nanoparticles improve the therapeutic efficacy and reduce the toxicity. We conclude GC4-targeted LPH nanoparticle formulation is a safe and effective delivery system for RNA-based therapy against metastatic melanoma.

## DISCUSSION

RNA-based therapeutics have recently been developed as a potential novel class of therapeutic agent to treat human diseases including cancer. RNA molecules such as siRNA and miRNA are highly effective therapies for cancer based on the ability to specifically silence the expression of cancer-related genes or to selectively regulate the pathways that are involved in the development and progression of malignancy. In this study, our delivery system provides an excellent platform to effectively, safely, and selectively deliver RNA-based therapeutics into the tumor.

Our study demonstrated that inhibition of c-Myc, MDM2, and VEGF protein expression by siRNA formulated with tumor-targeting scFv modified LPH nanoparticles significantly suppressed B16F10 metastatic tumor growth (Figures 3 and 4). Through co-delivery of miRNA and siRNA in the LPH formulation, the combination strategy is effective to trigger an enhanced therapeutic effect. To our knowledge, it is the first study of systemic delivery of miRNA for cancer therapy by using a targeted gene delivery system.

Many strategies were developed to treat cancer by targeting the cancer cells without affecting normal cells. Our results demonstrated that the formulation modified with tumor-targeting scFv is highly effective for delivery of siRNA or miRNA into the B16F10 lung metastasis. scFv has several advantages over the conventional monoclonal antibody or small molecule as a target moiety for drug/gene delivery to cancer. They include profound penetration into the tumor site, high specificity, strong affinity, low toxicity, and weak induction of the unwanted immune response. Nanoparticles modified with GC4 scFv may be internalized by the cells through receptor-mediated endocytosis. The cell-surface antigen associated with the B16F10 tumor to which GC4 scFv targets was not characterized in this study. However, once identified, the tumor-associated antigen could become a new target for cancer therapy.

miRNA, a potential therapeutic agent, regulates cellular behavior via specific targeting and downregulating mRNAs by nearly perfect base pairing.<sup>20</sup> It has been reported that certain miRNAs are involved in the oncogenic and tumor suppressor networks and can potentially inhibit tumorigenesis.<sup>21</sup> The miR-34a was found to suppress tumor proliferation and migration and cause apoptosis in cancer cells by activating p53 and downregulating c-Met and E2F3 (refs. 6–8). In this study, we found that miR-34a induced apoptosis, suppressed the survivin expression and inactivated MAPK pathway in B16F10 melanoma cells. Unlike other reports, we found the expression of c-Met was unaffected after transfection of miR-34a (data not shown). The signaling molecule upstream of MAPK pathways, which were downregulated by miR-34a, require further investigation.

The LPH nanoparticle formulation for RNA-based cancer therapy is potentially suitable for clinical use due to its reduced toxicity.<sup>22</sup> In addition, the ability of the nanoparticles to target tumor site further increases the therapeutic value of the RNA therapeutics. The capacity to deliver siRNA and/or miRNA with a single formulation simultaneously targeting several different oncogenic pathways is definitely an important advantage of the current approach. As far as we know, this is also the first report of co-delivery of miRNA and siRNA as cancer therapeutic agents. The delivery system makes it possible to evaluate the function of different therapeutic siRNAs or miRNAs both *in vitro* and in animal models. Such results would contribute to the basic cancer research and to the development of potential therapeutic agent.

## MATERIALS AND METHODS

**Materials.** DOTAP, cholesterol, DSPE-PEG<sub>2000</sub>, and DSPE-PEG<sub>2000</sub>-maleimide (DSPE-PEG-mal) were purchased from Avanti Polar Lipids (Alabaster, AL). Protamine sulfate (fraction X from salmon) and HA sodium salt from *Streptococcus equi* were obtained from Sigma-Aldrich (St Louis, MO). B16F10 cells, obtained from American Type Culture Collection, Manassas, VA, were widely used to establish an experimental lung metastasis model. The cells stably expressed GL3 firefly luciferase were created via retrovirus-mediated gene transduction in Pilar Blancafort's laboratory at the University of North Carolina at Chapel Hill. The cells were maintained in Dulbecco's modified Eagle's medium (Invitrogen, Carlsbad, CA) supplemented with 10% fetal bovine serum (Invitrogen). Antibodies conjugated with horseradish peroxidase (HRP) (mouse monoclonal antibodies against mouse MDM2, c-Myc, and rabbit polyclonal antibodies against VEGF), primary antibodies (mouse monoclonal antibodies against pERK and  $\beta$ -actin and rabbit polyclonal antibodies against survivin and ERK), and secondary antibodies conjugated with HRP (goat anti-mouse IgG-HRP and goat anti-rabbit IgG-HRP) were purchased from Santa Cruz Biotechnologies (Santa Cruz, CA). Primary antibody against Melan A was purchased from Abcam (Cambridge, MA). Monoclonal mouse antihexahistidine antibody was purchased from AbD Serotec/MorphoSys (Raleigh, NC). Phycoerythrin (PE)-conjugated goat anti-mouse IgG was purchased from Jackson ImmunoResearch (West Grove, PA). MDM2 siRNA (target sequence: 5'-GCUUCGGAACAAGAGACUC-3'), c-Myc siRNA (target sequence: 5'-GAACAUCAUCAUCCAGGAC-3'), VEGF siRNA (target sequence: 5'-CGAUGAAGCCCUGGAGUGC-3'), control siRNA (target sequence: 5'-AATTCTCCGACGTGTACAGT-3'), miR-34a (mature miRNA sequence: 5'-UGGCAGUGUCUUAGCUGGUUGU-3'), and control miRNA (mature miRNA sequence: 5'-UUGUACUACAAAA GUACUG-3') were purchased from Dharmacon (Lafayette, CO).

**Experimental animals.** Female C57BL/6 mice of ages 6–7 weeks (weights 16–18 g) were purchased from National Cancer Institute. All experiments performed with animals were in accordance with and approved by the Institutional Animal Care and Use Committee at the University of North Carolina. C57BL/6 mice were i.v. injected with  $2 \times 10^5$  B16F10 cells to establish experimental lung metastasis.

**Screening human scFvs binding to B16F10 cells.** A panel of internalizing tumor-targeting scFvs that were identified from previous studies<sup>13,23–26</sup> was tested for binding to B16F10 cells by FACS. ScFvs bearing a hexahistidine tag were incubated with  $10^5$  B16F10 cells at RT for 1 hour, washed twice with PBS/0.5% fetal bovine serum, and bound scFvs were detected by mouse anti-hexahistidine followed by goat anti-mouse-PE. The cells were analyzed by FACS LSR II (BD Biosciences, San Jose, CA). For control, a parallel incubation with B16F10 was set up with secondary detection agents only.

**Expression and purification of recombinant scFv bearing a C-terminal cysteine.** Genes encoding the GC4 scFv were subcloned from the phage vector into a pUC119-based secretion vector resulting in the addition of a cysteine and a hexahistidine tag to the c-terminus of the scFv as described.<sup>27,28</sup> Antibody fragments were harvested from the bacterial periplasm and purified using AKTAPrime (GE Healthcare, Piscataway, NJ) by immobilized metal affinity chromatography (IMAC, HiTrap His; GE Healthcare) and gel filtration (PD10; GE Healthcare). Purity was analyzed by 10% SDS-PAGE under both reducing and nonreducing conditions, and scFv concentrations were determined by NanoDrop (Thermo Scientific, Waltham, MA).

**Preparation of LPH nanoparticles modified with scFv.** The procedure of the formulation preparation was described earlier.<sup>22</sup> Briefly, cationic liposomes composed of DOTAP and cholesterol (1:1 molar ratio) were prepared by thin film hydration followed by membrane extrusion to reduce the particle size. To prepare LPH, 18  $\mu$ l of protamine (2 mg/ml), 140  $\mu$ l of deionized water, and 24  $\mu$ l of a mixture of siRNA or miRNA and HA (2 mg/ml) were mixed and kept at room temperature for 10 minutes before adding 60  $\mu$ l of cationic liposome (20 mmol/l). After 10 minutes at room temperature, LPH was mixed with 37.8  $\mu$ l of DSPE-PEG-mal (10 mg/ml) and incubated at 50–60 °C for 10 minutes. For scFv conjugation, scFv dimer was reduced using immobilized TCEP disulfide reducing gel (Thermo Scientific) according to manufacturer's recommendations, incubated with LPH nanoparticles containing DSPE-PEG-mal for 2 hours at room temperature, and the unreacted maleimide groups were quenched by adding L-cysteine.

**Cellular uptake study.** B16F10 cells were seeded on glass coverslips in 12-well plates (Corning, Corning, NY) 12 hours before experiments. Cells were treated with different formulations at a concentration of 250 nmol/l FITC-labeled siRNA in serum-containing medium at 37 °C for 1 hour. Cells were washed twice with PBS, counterstained with DAPI and imaged using a Leica SP2 confocal microscope (Leica Microsystems, Bannockburn, IL).

**Tissue distribution study.** B16F10 metastasis-bearing mice were given i.v. injections of FITC-labeled siRNA formulated in the nanoparticles on day 17. After 4 hours, mice were killed, and tissues were collected and homogenized in lysis buffer and incubated at room temperature for 30 minutes. The supernatant was collected after centrifugation at 14,000 rpm for 10 minutes, and 50  $\mu$ l supernatant was transferred to a black 96-well plate (Corning). The fluorescence intensity of the sample was measured by a plate reader (Bioscan, Washington, DC) at excitation wavelength 485 nm and emission wavelength 535 nm. siRNA concentration in each sample was calculated from a standard curve.

**Gene silencing study and apoptosis analysis in vitro.** B16F10 cells were seeded into 6-well plates at a concentration of  $2 \times 10^5$  per ml 24 hours before transfection. The cells were further transfected with miR-34a or a control

miRNA at a final concentration of 100 nmol/l using Lipofectamine 2000 (Invitrogen) according to the manufacturer's recommendations. Cells were harvested for the western blot assay and the analysis of apoptosis 72 hours after transfection. Apoptosis was analyzed by annexin V staining. Briefly,  $1 \times 10^5$  cells were harvested 72 hours after transfection and resuspended in 100  $\mu$ l binding buffer containing 5  $\mu$ l annexin V-FITC (BD Biosciences) for 15 minutes at room temperature in the dark. The Annexin V positive cells were analyzed by flow cytometry.

**Gene silencing study in lung metastasis.** B16F10 metastasis-bearing mice were given i.v. injections of the combined siRNA or miRNA formulated in the nanoparticles on days 10 and 11. Twenty-four hours after the second injection, the mice were killed, and the tumor-loaded lungs were collected for the immunostaining or western blot analysis. Expressions of MDM2, c-Myc, and VEGF in the sections were examined immunostaining using the first antibodies against three different proteins and FITC-secondary antibodies against mouse or rabbit IgG. The slides were imaged by using a Leica SP2 confocal microscope. For western blotting, total protein (10  $\mu$ g) isolated from the tumor-loaded lung was electrophoresed in a polyacrylamide/sodium dodecyl sulfate gel and transferred to a PVDF membrane. The membrane was blocked with 5% nonfat milk in phosphate-buffered saline for 1 hour and then incubated overnight with primary antibody at 4 °C. After the membrane had been washed with PBST (0.1% Tween 20 in PBS) five times, it was further incubated with the HRP-conjugated secondary antibody for 1 hour. The membrane was washed and developed with enhanced chemiluminescence using ECL plus (GE Healthcare, Little Chalfont, UK) followed by autoradiography.

**TUNEL assay.** TUNEL staining was performed as recommended by the manufacturer's protocol (Promega, Madison, WI). B16F10 metastasis-bearing mice were given i.v. injections of the miRNA formulated in the nanoparticles on days 10 and 11. Twenty-four hours after the second injection, the mice were killed, and the tumor-loaded lungs were collected for the TUNEL staining. Images from TUNEL-stained tumor sections were captured with Nikon ECLIPSE Ti-U microscopy (Nikon Instruments, Melville, NY).

**In vivo tumor growth/metastasis inhibition study.** B16F10 metastasis-bearing mice were i.v. injected with siRNA or miRNA in the nanoparticles on days 8 and 9. On day 19, the mice were killed, and the tumor-loaded lungs were collected. For quantification of the lung metastasis nodules, one lobe per lung was analyzed for luciferase activity. The lung lobe was homogenized in 0.2 ml of lysis buffer (0.05% Triton X-100 and 2 mmol/l EDTA in 0.1 mol/l Tris-HCl) followed by centrifugation at 13,000 rpm for 10 minutes. Ten microliters of the supernatant were mixed with 90  $\mu$ l of luciferase substrate (Luciferase Assay System; Promega), and the luciferase activity was measured by a plate reader (Bioscan). The collected lobe was further fixed in 10% formalin for hematoxylin and eosin staining.

**Statistical analysis.** All statistical analyses were performed by Student's *t*-test.

## SUPPLEMENTARY MATERIAL

**Figure S1.** Uptake of siRNA *in vitro*.

### Materials and Methods.

## ACKNOWLEDGMENTS

We thank Michael Hooker Microscopy Facility at the University of North Carolina (UNC) for the microscopy images. This research was supported by National Institutes of Health grants CA129825, CA135586, and CA118919, and by the UNC at Chapel Hill, Chapel Hill, NC and the University of California at San Francisco, San Francisco, CA.

## REFERENCES

1. Castanotto, D and Rossi, JJ (2009). The promises and pitfalls of RNA-interference-based therapeutics. *Nature* **457**: 426–433.



2. Coburn, GA and Cullen, BR (2003). siRNAs: a new wave of RNA-based therapeutics. *J Antimicrob Chemother* **51**: 753–756.
3. Lu, J, Getz, G, Miska, EA, Alvarez-Saavedra, E, Lamb, J, Peck, D *et al.* (2005). MicroRNA expression profiles classify human cancers. *Nature* **435**: 834–838.
4. Li, SD, Chono, S and Huang, L (2008). Efficient oncogene silencing and metastasis inhibition via systemic delivery of siRNA. *Mol Ther* **16**: 942–946.
5. Gou, D, Zhang, H, Baviskar, PS and Liu, L (2007). Primer extension-based method for the generation of a siRNA/miRNA expression vector. *Physiol Genomics* **31**: 554–562.
6. Yan, D, Zhou, X, Chen, X, Hu, DN, Dong, XD, Wang, J *et al.* (2009). MicroRNA-34a inhibits uveal melanoma cell proliferation and migration through downregulation of c-Met. *Invest Ophthalmol Vis Sci* **50**: 1559–1565.
7. Li, Y, Guessous, F, Zhang, Y, Dipierro, C, Kefas, B, Johnson, E *et al.* (2009). MicroRNA-34a inhibits glioblastoma growth by targeting multiple oncogenes. *Cancer Res* **69**: 7569–7576.
8. Welch, C, Chen, Y and Stallings, RL (2007). MicroRNA-34a functions as a potential tumor suppressor by inducing apoptosis in neuroblastoma cells. *Oncogene* **26**: 5017–5022.
9. Hammond, SM (2006). MicroRNA therapeutics: a new niche for antisense nucleic acids. *Trends Mol Med* **12**: 99–101.
10. Krützfeldt, J, Rajewsky, N, Braich, R, Rajeev, KG, Tuschl, T, Manoharan, M *et al.* (2005). Silencing of microRNAs *in vivo* with ‘antagomirs’. *Nature* **438**: 685–689.
11. Li, SD, Chen, YC, Hackett, MJ and Huang, L (2008). Tumor-targeted delivery of siRNA by self-assembled nanoparticles. *Mol Ther* **16**: 163–169.
12. Chen, Y, Sen, J, Bathula, SR, Yang, Q, Fittipaldi, R and Huang, L (2009). Novel cationic lipid that delivers siRNA and enhances therapeutic effect in lung cancer cells. *Mol Pharm* **6**: 696–705.
13. Zhu, X, Bidlingmaier, S, Hashizume, R, James, CD, Berger, MS and Liu, B. Identification of internalizing human single chain antibodies targeting brain tumor sphere cells. *Mol Cancer Ther*, in the press.
14. Xia, J, Bi, H, Yao, Q, Qu, S and Zong, Y (2006). Construction of human ScFv phage display library against ovarian tumor. *J Huazhong Univ Sci Technol Med Sci* **26**: 497–499.
15. Tsantili, P, Tzartos, SJ and Mamalaki, A (1999). High affinity single-chain Fv antibody fragments protecting the human nicotinic acetylcholine receptor. *J Neuroimmunol* **94**: 15–27.
16. Chen, Z, Liang, K, Liu, J, Xie, M, Wang, X, Lü, Q *et al.* (2009). Enhancement of survivin gene downregulation and cell apoptosis by a novel combination: liposome microbubbles and ultrasound exposure. *Med Oncol* **26**: 491–500.
17. Takeuchi, H, Morton, DL, Elashoff, D and Hoon, DS (2005). Survivin expression by metastatic melanoma predicts poor disease outcome in patients receiving adjuvant polyvalent vaccine. *Int J Cancer* **117**: 1032–1038.
18. Fecher, LA, Amaravadi, RK and Flaherty, KT (2008). The MAPK pathway in melanoma. *Curr Opin Oncol* **20**: 183–189.
19. Li, N, Fu, H, Tie, Y, Hu, Z, Kong, W, Wu, Y *et al.* (2009). miR-34a inhibits migration and invasion by down-regulation of c-Met expression in human hepatocellular carcinoma cells. *Cancer Lett* **275**: 44–53.
20. Tsuchiya, S, Okuno, Y and Tsujimoto, G (2006). MicroRNA: biogenetic and functional mechanisms and involvements in cell differentiation and cancer. *J Pharmacol Sci* **101**: 267–270.
21. Ruvkun, G (2006). Clarifications on miRNA and cancer. *Science* **311**: 36–37.
22. Chono, S, Li, SD, Conwell, CC and Huang, L (2008). An efficient and low immunostimulatory nanoparticle formulation for systemic siRNA delivery to the tumor. *J Control Release* **131**: 64–69.
23. Ruan, W, Sassooun, A, An, F, Simko, JP and Liu, B (2006). Identification of clinically significant tumor antigens by selecting phage antibody library on tumor cells *in situ* using laser capture microdissection. *Mol Cell Proteomics* **5**: 2364–2373.
24. An, F, Drummond, DC, Wilson, S, Kirpotin, DB, Nishimura, SL, Broaddus, VC *et al.* (2008). Targeted drug delivery to mesothelioma cells using functionally selected internalizing human single-chain antibodies. *Mol Cancer Ther* **7**: 569–578.
25. Bidlingmaier, S, He, J, Wang, Y, An, F, Feng, J, Barbone, D *et al.* (2009). Identification of MCAM/CD146 as the target antigen of a human monoclonal antibody that recognizes both epithelioid and sarcomatoid types of mesothelioma. *Cancer Res* **69**: 1570–1577.
26. Conrad, F, Zhu, X, Zhang, X, Chalkley, RJ, Burlingame, AL, Marks, JD *et al.* (2009). Human antibodies targeting cell surface antigens overexpressed by the hormone refractory metastatic prostate cancer cells: ICAM-1 is a tumor antigen that mediates prostate cancer cell invasion. *J Mol Med* **87**: 507–514.
27. Liu, B, Conrad, F, Cooperberg, MR, Kirpotin, DB and Marks, JD (2004). Mapping tumor epitope space by direct selection of single-chain Fv antibody libraries on prostate cancer cells. *Cancer Res* **64**: 704–710.
28. Roth, A, Drummond, DC, Conrad, F, Hayes, ME, Kirpotin, DB, Benz, CC *et al.* (2007). Anti-CD166 single chain antibody-mediated intracellular delivery of liposomal drugs to prostate cancer cells. *Mol Cancer Ther* **6**: 2737–2746.